C.P. No. 696
C.P. No. 696

MINISTRY OF AVIATION

AERONAUTICAL RESEARCH COUNCIL

CURRENT PAPERS

Turbulent Boundary Layers on Delta Wings at Zero Lift

by

J. C. Cooke D.Sc.

LONDON: HER MAJESTY'S STATIONERY OFFICE

1963

FIVE SHILLINGS NET

U.D.C. No. 533.693.3 : 532.526.4 : 533.6.011.5

C.P. No. 696

March, 1963

TURBULENT BOUNDARY LAYERS ON DELTA WINGS AT ZERO LIFT

by

J. C. Cooke, D.Sc.

SUMMARY

It is found that, for turbulent flow at Mach number 2 over a thin delta wing at zero lift, the effect of pressure gradient on the boundary layer is negligible; thus boundary layer calculations allowing for convergence and divergence of streamlines are simplified. When these are done it is found that, except near the centre line, where streamline convergence causes extra thickening towards the trailing edge, the momentum thickness is nearly the same as it would be for flow over a flat plate of the same planform. This enables the boundary layer pressure drag and the skin friction drag to be determined simply. It is found that the pressure drag may be neglected compared with the total drag, whilst the skin friction is the same as that of a flat plate of the same planform.

Replaces R.A.E. Tech. Note No. Aero. 2878 - A.R.C. 24,884

LIST OF CONTENTS

		Page
1	INTRODUCTION	4
2	THE WINGS CONCERNED	5
3	EFFECT OF PRESSURE GRADIENT IN TWO DIMENSIONAL CALCULATIONS	6
4	THE SHAPE OF THE EXTERNAL STREAMLINES	8
5	THE EFFECT OF STREAMLINE CONVERGENCE OR DIVERGENCE	8
6	SOME ACTUAL MAGNITUDES IN A TYPICAL CASE	10
7	THE EFFECT ON THE PRESSURE DISTRIBUTION	10
8	THE BOUNDARY LAYER PRESSURE DRAG	12
9	THE SKIN FRICTION DRAG	13
10	CONCLUSIONS	14
LIST OF SYMBOLS		15
LIST OF REFERENCES		17
APPENDIX 1 - Determination of $\Delta\phi$ and Δc_p		18 to 20
TABLES 1-4		-
ILLUSTRATIONS - Figs.1-5		-
DETACHABLE ABSTRACT CARDS		-

LIST OF TABLES

Table			
1	-	Values of constants in Spence's equation. Zero heat transfer	7
2	-	Boundary layer thicknesses at the trailing edge	10
3	-	Value of $K(\eta)$ for $\ell = 0{\cdot}8$	11
4	-	Drag coefficients for the wing tested by Firmin	13

LIST OF ILLUSTRATIONS

	Fig.
Values of $(\theta/c)^{1\cdot 2}$ by two dimensional calculations	1
Calculated external streamlines Nos. 1-5	2
Values of $(\theta/c)^{1\cdot 2}$ along streamlines 1-5	3
Isobars of Δc_p for $R = 10^7$, $\beta s/c = 0\cdot 577$	4
Δc_p where $y/s = 0\cdot 225$, by simple wave and slender wing theories	5

1 INTRODUCTION

In an attempt to assess the effect of the boundary layer on the drag of slender wings at zero lift, turbulent boundary layer calculations are made for a certain delta wing which has been tested at Bedford, using the measured pressure distribution and, in cases where this does not give enough information, using also calculated cross velocity components.

Firstly a simple calculation is made by Spence's method[1] assuming the flow to be two-dimensional along a series of chordwise sections. This clearly shows that the pressure gradients on the wing are so small that the boundary layer (calculated on the very simple two-dimensional basis) behaves almost exactly as though the pressure gradient were zero everywhere, that is, as though the flow were over a flat plate. This simplifies the subsequent work since the pressure gradients can be ignored leaving it possible to concentrate on the effect of diverging or converging streamlines. The wing concerned had an 11% thickness chord ratio. For thinner wings one may expect this conclusion to be even more justified.

A second set of calculations is then made. It consists of two parts - firstly the determination of the external streamlines, and secondly the calculation of boundary layer momentum thickness along these streamlines, allowing for convergence but not for pressure gradient. It is found that, except for streamlines very near to the centre line, the momentum thickness is still very close to what it would have been on the flat plate assumption. Near the centre line convergence of the streamlines causes considerable thickening of the boundary layer towards the rear, but this effect decreases very rapidly as we go outboard.

The next step, therefore, is to ignore the effect of convergence and to assume that the momentum thickness and displacement thickness over the wing are the same as over a flat plate. Thus a displacement surface is very simply obtained and the effect of this on the velocity potential ϕ is expressed in terms of an added function $\Delta\phi$; thus Δc_p, the increase in the pressure coefficient, can be calculated, and isobars of Δc_p may be plotted.

Finally by integration over the surface of the wing the boundary layer normal pressure drag coefficient is found. This drag is positive in the first example under consideration but it is very small. In fact its value at Mach number 2 and Reynolds number 10^7 is 0·00008. At higher Reynolds numbers it will of course be less than this. The calculated inviscid wave drag coefficient is 0·00821; thus the boundary layer pressure drag is 1% of the inviscid wave drag. This indeed may be an overestimate, since it assumes a displacement thickness which, as has already been pointed out, is too small at the rear near to the centre line. This increased thickness here will give an increased c_p, which, being on backward facing surfaces, will reduce the drag. This effect, however, only occurs over a narrow band and so the reduction will be small. It seems unlikely to be sufficient in this example to give negative drag, though this could possibly happen in other examples.

As already pointed out, the wing on which these calculations were made had a maximum thickness chord ratio of over 11%. For thinner wings one might expect the flow to be even closer to that over a flat plate. The same line of approach may be used for other planforms besides deltas, though the analysis in such cases would be more difficult.

Formulae are given which enable Δc_p to be determined at any point of any slender thin delta wing at zero lift at any Mach number or Reynolds number. Thus by integration the boundary layer pressure drag of the wing can be calculated. The skin friction will be the same as that over a flat plate, or possibly slightly less in the present example owing to the behaviour of the momentum thickness near to the centre line. The main conclusion, however, is that the boundary layer pressure drag is small and may probably be neglected at full scale. A second example was considered later and for this there is a reduction in pressure drag which amounts to 3% at $R = 10^7$, due to the thickness of the boundary layer.

The flow is supposed to be compressible and everywhere turbulent. If there are areas of both laminar and turbulent flow the calculation of Δc_p is more difficult; another complication is the sudden decrease in displacement thickness which occurs at transition owing to the sudden drop in the value of the shape factor H which takes place, whilst the momentum thickness remains continuous[2]. Since at full scale the flow is likely to be turbulent over most of the wing we do not consider here the case in which it is partly laminar.

The work done here only applies to wings at zero lift. At higher incidences it seems probable that the method of simplification given here would not be possible; it may be so, however, if the flow is attached along the leading edges of a cambered wing at a low lift coefficient.

There seems to be no check on this theory by experiment as yet. This would be a difficult undertaking, but accurate measurement of a few boundary layer profiles on the surface of the wing near to the trailing edge would be of great help.

2 THE WINGS CONCERNED

Two examples were used. These were both of delta plan form and had equations

$$z = \pm \frac{7V}{2sc}\left\{4 - 10\frac{x}{c} + 10\left(\frac{x}{c}\right)^2 - 5\left(\frac{x}{c}\right)^3 + \left(\frac{x}{c}\right)^4\right\}\left(\frac{x}{c} - \left|\frac{y}{s}\right|\right),$$

$$s/c = 1/3 \quad , \qquad V = 0{\cdot}01\, c^2 ,$$

known as the "Lord V" wing, which was tested at Bedford, and

$$z = \pm \frac{c}{240}\left\{42 + 116\frac{x}{c} - 660\left(\frac{x}{c}\right)^2 + 852\left(\frac{x}{c}\right)^3 - 350\left(\frac{x}{c}\right)^4\right\}\left(\frac{x}{c} - \left|\frac{y}{s}\right|\right),$$

$$s/c = 1/4 ,$$

which was tested at Farnborough by Firmin[3], who named it Wing 3. This wing is such that at the trailing edge

$$\frac{S'(1)}{c} \Big/ \frac{V}{c^3} = -16 ,$$

where $S(x/c)$ is the cross sectional area and V is the total volume.

Here s is the semi-span at the trailing edge and c the root chord.

In the case of the Lord V wing agreement between calculations of pressure distribution by slender wing theory was good. This did not apply to the second wing and so calculations were made for it by Firmin by linear wing theory. He found that this theory gave fair agreement with his experiments. This gives ground for the hope that the calculated values of ϕ_y and ϕ_{yy} of necessity used in Section 5 below may not be too much in error. The second wing has large backwards facing slopes at the rear and thus cannot be considered "slender".

3 EFFECT OF PRESSURE GRADIENT IN TWO-DIMENSIONAL CALCULATIONS

A cartesian co-ordinate system is used, the median plane of the wing being $z = 0$, with the x-axis along the centre line. The equation of the wing surface is $z = z(x,y)$ as in Section 2, and $\partial z/\partial x$ and $\partial z/\partial y$ are supposed small.

We choose the method of Spence[1]. In the absence of a shock the equation for the momentum thickness θ in a turbulent boundary layer may be written

$$\left(\frac{\theta}{c}\right)^{1+\frac{1}{n}} \left(\frac{u_e}{u_\infty}\right)^{B+\frac{1}{n}} \left(\frac{T_e}{T_\infty}\right)^{D} R^{\frac{1}{n}} = \frac{n+1}{n} C \int \left(\frac{T_e}{T_\infty}\right)^{E} \left(\frac{T_m}{T_e}\right)^{-P} \left(\frac{u_e}{u_\infty}\right)^{B} d\left(\frac{x}{c}\right) + \text{constant} . \qquad \ldots.(1)$$

In this equation the subscripts e, ∞ and m refer to values at the edge of the boundary layer, at infinity and at a certain "mean" position respectively. R, the Reynolds number, is equal to $u_\infty c/\nu_\infty$.

Depending on the ranges of $R_\theta (= u_e\theta/\nu_e)$ concerned (which overlap) n may take the values 4, 5 or higher values. We give in Table 1 the values of the constants for zero heat transfer when $n = 4$ and $n = 5$.

TABLE 1

Values of constants in Spence's equation. Zero heat transfer

	$n = 4$	$n = 5$
C	0·0128	0·00885
$\frac{n+1}{n} C$	0·0160	0·0106
B	4·125	4·0
D	1·735	1·665
E	1·332	1·343
P	0·778	0·822
H	$2{\cdot}5(1+0{\cdot}178M^2)-1$	
T_m/T_e	$1+0{\cdot}128M^2$	
Range of R_θ	100-5000	500-50,000

The value n = 5 was chosen for the first calculations. Taking the measured pressure distribution at various values of y/s for the first wing at Mach number 2 and Reynolds number 10^7, based on root chord, the solutions in Fig.1 were obtained (circles).

If there had been no pressure gradient, so that $u_e = u_\infty$, $T_e = T_\infty$, $M = M_\infty$, as on a flat plate, equation (1) on integration would have reduced to

$$\left(\frac{\theta}{c}\right)^{1+\frac{1}{n}} = \frac{n+1}{n} C R^{-\frac{1}{n}} \left(1 + 0{\cdot}128M_\infty^2\right)^{-P} \left(\frac{x}{c} - \left|\frac{y}{s}\right|\right), \tag{2}$$

assuming θ to vanish at the leading edge, which will be the case if this edge is sharp.

For $R = 10^7$, $M_\infty = 2$, $n = 5$ equation (2) becomes

$$\left(\frac{\theta}{c}\right)^{1\cdot 2} = 0{\cdot}000300 \left(\frac{x}{c} - \left|\frac{y}{s}\right|\right), \tag{3}$$

or, for n = 4

$$\left(\frac{\theta}{c}\right)^{1\cdot 25} = 0{\cdot}000206 \left(\frac{x}{c} - \left|\frac{y}{s}\right|\right), \tag{4}$$

$\left(\frac{\theta}{c}\right)^{1\cdot 2}$ obtained by equation (3) is plotted for the first example as a full line in Fig.1 for comparison with the results with pressure gradient. As can be seen the result is scarcely distinguishable from that obtained by a full solution of equation (1). Equation (4) gives results virtually coincident with those of equation (3). The same conclusions apply to the second example.

Thus we may say that the measured pressure gradient of the wing at zero lift is so small as to be negligible in boundary layer calculations. This may not always be true. The equation from which (1) is derived is

$$\frac{d\theta}{dx} + \frac{\theta}{u_e} \frac{\partial u_e}{\partial x}\left(2 + H - M^2\right) = \frac{\tau}{\rho_e u_e^2}$$

and the effect of the pressure gradient lies in the second term. (It must also affect τ to some extent but this is generally ignored.) Now from Table 1

$$2 + H - M^2 = 3 \cdot 5 - 0 \cdot 555 M^2$$

and this vanishes when $M = 2 \cdot 51$, which is not very far away from the value $M = 2$ used in the calculations. At any rate we have shown that the pressure gradient has very little effect in our examples and we shall ignore it from now onwards.

4 THE SHAPE OF THE EXTERNAL STREAMLINES

The streamlines are calculated from the equation

$$\frac{dy}{dx} = \frac{v_e}{u_e}, \tag{5}$$

where u_e and v_e are the x and y components of the external velocity. Only the value of u_e can be obtained from the measured pressure distribution and so v_e was found by a slender thin wing calculation for the given wing. The solution of equation (5) is straightforward but involves some interpolation and iteration. If v_e is calculated for a few values of y/s near to the particular one concerned the interpolation can be done graphically. Once y is found, ϕ_{yy} (which is required in later calculations) may also be found by interpolation.

Some of the streamlines for the first example are shown in Fig.2. They diverge near to the leading edge but converge later. However, the convergence is very slight except near to the centre line. This convergence is very much less in the second example.

5 THE EFFECT OF STREAMLINE CONVERGENCE OR DIVERGENCE

According to the axi-symmetric analogy[4] the boundary layer along any streamline on the wing $z = z(x,y)$ behaves like that over an axially symmetric body of radius r, where r is given by

$$U_e \frac{\partial}{\partial s}\left(\log r^2 U_e^2\right) = 2\left(\frac{\partial u_e}{\partial x} + \frac{\partial v_e}{\partial y}\right), \tag{6}$$

assuming that $\partial z/\partial x$ and $\partial z/\partial y$ are small. Here we have written $U_e^2 = u_e^2 + v_e^2$ and s represents distance measured along a streamline.

Hence we have

$$\frac{U_e}{r}\frac{\partial r}{\partial s} = \frac{\partial v_e}{\partial y} \tag{7}$$

ignoring the velocity gradient $\partial U_e/\partial s$ and ignoring also $\partial u_e/\partial x$ compared with $\partial v_e/\partial y$ in accordance with the usual slender body theory. In any case $\partial u_e/\partial x$ is approximately equal to $\partial U_e/\partial s$ which we have already decided to ignore.

If the external perturbation potential is $u_\infty \phi$ and we write $U_e = u_\infty$, equation (7) becomes

$$\frac{1}{r}\frac{\partial r}{\partial s} = \phi_{yy} . \tag{8}$$

Now Spence[1] gives the form of his equation for an axi-symmetric body. It is the same as equation (1) except that $r^{1+1/n}$ is to be inserted in the left hand side and also inside the integral on the right hand side. In using the axi-symmetric analogy we must follow a streamline and hence $d(x/c)$ should be replaced by $d(s/c)$. We must also replace u_e by U_e. As we are ignoring the pressure gradient we shall write $U_e = u_\infty$, $T_e = T_\infty$, $M = M_\infty$. It is more convenient to differentiate the equation. Using the version $n = 5$ in Table 1 and writing $\Theta = (\theta/c)^{1\cdot 2}$ we find

$$\frac{d\Theta}{d(s/c)} + 1\cdot 2\,\frac{1}{r}\,\frac{\partial r}{\partial(s/c)} = 0\cdot 0106\ R^{-0\cdot 2}\,(1 + 0\cdot 128 M_\infty^2)^{-0\cdot 822} ,$$

or, for $M_\infty = 2$, $R = 10^7$, using equation (8)

$$\frac{d\Theta}{d(x/c)} + 1\cdot 2\ c\ \phi_{yy}\,\Theta = 0\cdot 000300 , \tag{9}$$

where we have replaced s/c by x/c, since the streamlines are nearly parallel to the x-axis.

If $\phi_{yy} = 0$ this equation has equation (3) as its solution, as was to be expected. Thus the effect of convergence or divergence of the streamlines is expressed by the term $1\cdot 2c\ \phi_{yy}\ \Theta$ in equation (9).

The solutions of equation (9) for the first example are shown in Fig.3 for various streamlines, numbered 1 to 5 in Fig.2, together with values from equation (3).

The main feature of the curves in Fig.3 is that the solutions by equation (9) and the flat plate solution run very near to each other, except near to the centre line, where the error in θ rises to about 50%. This is, however, confined to an area very near to the centre line. At other locations the initial divergence reduces the value of Θ slightly and the convergence which occurs downstream has little effect on Θ. Consequently in calculating the effect of displacement on pressure drag we may assume flat plate values and expect that the error near to the centre line will only have a small effect on the total drag. In the second example the values are closer together, the extra thickness only rising to about 5% near the centre line.

6 SOME ACTUAL MAGNITUDES IN A TYPICAL CASE

It may be of interest to give some idea of the actual magnitudes of the various boundary layer thicknesses near the trailing edge of a full-scale wing. We consider a delta wing with a root chord of 200 feet, flying at a Mach number of 2·2 at a height of 55,000 feet. θ is obtained from the first example whilst δ^* and δ are found on the assumption that the velocity in the boundary layer follows a 1/7th power law. It has been assumed of course that the boundary layer is turbulent all over the wing, and that there is zero heat transfer.

TABLE 2

Boundary layer thicknesses at the trailing edge

y/s	θ	δ^*	δ
0·05	4·1"	14·5"	55·7"
0·2	2·3"	8·2"	31·2"
0·5	1·6"	5·5"	21·1"
0·8	0·7"	2·6"	9·8"

7 THE EFFECT ON THE PRESSURE DISTRIBUTION

Putting c = 1 for convenience we may take the momentum thickness θ to be given by

$$\theta^{1+\frac{1}{n}} = \frac{1+n}{n} C \left(x - \left|\frac{y}{s}\right|\right) R^{-\frac{1}{n}} \left(1 + 0{\cdot}128 M_\infty^2\right)^{-\beta} ,$$

no allowance being made for convergence or divergence of streamlines. C and β are given in Table 1 for values n = 4 or n = 5. We shall choose n = 4 as being slightly simpler numerically, with no loss in accuracy.

Since
$$\delta^* = H\theta$$

where H is given in Table 1, we have

$$\delta^* = 0{\cdot}0370 \left\{2{\cdot}5\left(1 + 0{\cdot}178 M_\infty^2\right) - 1\right\} \left(x - \left|\frac{y}{s}\right|\right)^{0\cdot 8} R^{-0\cdot 2} \left(1+0{\cdot}128 M_\infty^2\right)^{-0\cdot 622} . \qquad \text{....(10)}$$

We shall write

$$\delta^* = L\left(x - \left|\frac{y}{s}\right|\right)^{\ell} \tag{11}$$

and note that for $\ell = 0{\cdot}8$ (corresponding to $n = 4$) $M_\infty = 2$, $R = 10^7$ we have $L = 0{\cdot}00374$.

The effect of the boundary layer on the flow is the same as though the fluid were inviscid, but that the wing $z = z(x,y)$ were replaced by

$$z = z(x,y) + \delta^*.$$

We shall use slender thin wing theory, which is a linear theory. Hence if $u_\infty\phi$ is the velocity potential due to $z(x,y)$ and $u_\infty\Delta\phi$ is that due to δ^* the two values may be added to obtain the overall velocity potential. $\Delta\phi$ is calculated in Appendix 1 by methods explained in Ref.5. We aim to determine Δc_p, the change in pressure coefficient due to displacement thickness.

The result for $\ell = 0{\cdot}8$, corresponding to $n = 4$, is, if

$$\eta = \frac{y}{sx} \quad , \qquad \beta^2 = M_\infty^2 - 1 \ ,$$

$$\Delta c_p = \frac{8L}{5\pi}\, sx^{-0\cdot 2}\left\{K(|\eta|) - 2\log\tfrac{1}{2}\beta s\right\} \ , \tag{12}$$

assuming as before that $C = 1$. The value of K is given in Table 3.

TABLE 3

Value of $K(\eta)$ for $\ell = 0{\cdot}8$

η	0·00	0·10	0·20	0·30	0·40	0·50	0·60
$K(\eta)$	0·000	0·004	0·023	0·063	0·130	0·233	0·388

η	0·70	0·75	0·80	0·85	0·90	0·95	1·00
$K(\eta)$	0·627	0·798	1·027	1·349	1·852	2·841	∞

In the first example, for which $s = 1/3$, $M_\infty = 2$, $R = 10^7$, $L = 0{\cdot}00374$ $\beta s = 0{\cdot}577$, Δc_p is always positive. Isobars of Δc_p are shown in Fig.4. These are likely to be reasonably accurate except in the rear part of the wing near to the centre line, where the increasing displacement thickness should cause an increase in Δc_p.

It may be noted that we may not suppose that Δc_p can be obtained from simple wave theory. We show in Fig.5 the value of Δc_p compared with that obtained by simple wave theory, along the line $y/s = 0{\cdot}225$. Similar divergences occur everywhere on the wing.

Δc_p has a singularity at $|\eta| = 1$. In fact when $\eta = 1-\varepsilon$ it can be shown that

$$K(1-\varepsilon) = 4{\cdot}3240\varepsilon^{-0{\cdot}2} - 5{\cdot}0606 + 0{\cdot}583\varepsilon + O(\varepsilon^2) , \tag{13}$$

and so the singularity is integrable.

8 THE BOUNDARY LAYER PRESSURE DRAG

Once Δc_p is known the boundary layer pressure drag coefficient is calculated from the formula

$$\Delta C_D = \frac{2}{s} \int_{-s}^{s} dy \int_{|y/s|}^{1} \Delta c_p \frac{\partial z}{\partial x} dx ,$$

taking into account both surfaces of the wing. Hence

$$\Delta C_D = 4 \int_{0}^{1} dk \int_{k}^{1} \Delta c_p \frac{\partial z}{\partial x} dx , \tag{14}$$

or writing $k = y/s$.

In our first example we evaluate the integral numerically using equation (13) near the singularity. We find for $R = 10^7$ that

$$\Delta C_D = 0{\cdot}00008 .$$

This is only 1% of the inviscid wave drag, which is $0{\cdot}00821$. The wing considered is rather thick (maximum thickness/chord ratio of $11{\cdot}2\%$) and the inviscid wave drag varies as the square of the thickness, whilst ΔC_D varies as the thickness. Hence if the maximum thickness of the wing were halved the inviscid drag would be reduced to one quarter the above value whereas ΔC_D would be halved. Hence ΔC_D would rise to 2% of the inviscid value. On the other hand ΔC_D varies as $R^{-0{\cdot}2}$ so that an increase in Reynolds number from 10^7 to full scale (say 4×10^8) has the effect of halving ΔC_D.

In the second example the pressure drag was directly calculated by the supersonic area rule. This drag was found to be negative and the reduction in drag thereby produced amounted to as much as $4{\cdot}3\%$ for a Reynolds number of 2×10^6. The results are given in Table 4. With a machine programme available it was possible to take into account the increased thickening of the boundary layer near to the centre line. It was found, however, to make no appreciable difference to the overall drag. These calculations were performed by J.A. Beasley, who devised the machine programme.

TABLE 4

Pressure drag coefficients for the wing tested by Firmin. $M = 2 \cdot 2$

R	C_D	Decrease due to boundary layer
∞	0·00562	-
10^7	0·00544	3·2%
6×10^6	0·00543	3·4%
2×10^6	0·00538	4·3%

9 THE SKIN FRICTION DRAG

For a thin wing with a boundary layer development as described above the total skin friction drag will be approximately the same as that over a flat plate with the same planform. A fair approximation to this may be found by assuming the plate to be rectangular with a chord equal to the mean chord of the wing. We may then find the drag in the manner recommended by Monaghan[6]. This gives an overall drag coefficient, taking both sides of the plate into consideration, of

$$C_F = 0 \cdot 92 \frac{T_e}{T_w} \left\{ \log_{10} R \left(\frac{T_e}{T_w} \right)^{2 \cdot 8} \right\}^{-2 \cdot 6} , \qquad (15)$$

where R is the Reynolds number based on mean chord and on free stream conditions and, in the case of zero heat transfer,

$$\frac{T_w}{T_e} = 1 + 0 \cdot 178 M_\infty^2 .$$

This gives for the wing discussed earlier, with a mean chord of 100 feet, flying at Mach 2·2 at 55,000 feet

$$C_F = 0 \cdot 00257 .$$

This will apply even if the wing varies in shape and thickness, so long as the Reynolds number, based on mean chord, is unchanged and the wing is thin and has a low lift coefficient with attached flow.

If the wing is a delta with rhombic cross-sections and Lord V area distribution and maximum thickness chord ratio 11·2% the wave drag coefficient is 0·00821, whilst for 5·6% thickness the coefficient is 0·00205. In the latter case the skin friction drag and wave drag are roughly of the same order of magnitude, whilst the boundary layer pressure drag is 0·5% of the total wave drag plus skin friction drag.

The streamline convergence towards the rear near to the centre line, ignored in the above estimates, will cause an increased pressure coefficient, and this, being on backwards facing surfaces, will reduce the pressure drag slightly in the first example. In the second example the change is negligible.

10 CONCLUSIONS

The main results are that at moderate Mach numbers:-

(1) The boundary layer over a thin delta wing at zero lift develops in much the same way as though the wing were a flat plate of the same planform placed edge on to the stream, and the skin friction is the same as that of a flat plate.

(2) At test and full scale Reynolds numbers the boundary layer normal pressure drag is in general small enough to be neglected compared with the inviscid wave drag and skin friction drag, though this may not be true for a wing with large slopes at the rear, as in our second example.

There seems to be no reason why these conclusions should not apply to other planforms besides deltas so long as the wings are slender and thin.

Little experimental evidence for these results is available; however it was found for the first example that the sum of the calculated inviscid wave drag of the wing and the skin friction of a flat plate of the same planform was in fair agreement with the measured overall drag the maximum error being about 2%. Agreement was not quite so good in the second example, the error being about 5%.

It is likely that the cause of the disagreement lies mainly in errors in the boundary layer part of the calculations. These ultimately depend on the assumption of some skin friction law for flow over a flat plate. In view of the small effect of pressure gradient which the calculations show, the use of flat plate laws may possibly be justified, but one must remember that Monaghan[6] did not claim better than 10% accuracy even for flat plate flows.

There are nevertheless other sources of error which should not be forgotten. One of these is the use of linear theory to determine the inviscid flow. In the first example considered here (Lord V) slender theory leads to quite accurate pressure distributions, but it does not do so for the second example (Firmin's Wing 3). Calculations by linear thin-wing theory give improved results for this case, but even so the measured pressure near to the trailing edge does not agree too well with calculations. Finally, one must bear in mind that in the experiments the bands of roughness put on near the leading edges to induce transition may provide yet another source of error, in spite of efforts made to allow for this.

If boundary layer profiles near to the trailing edges of slender wings were measured at a number of spanwise stations it might be possible to obtain further verification of the suggestions here presented.

LIST OF SYMBOLS

a,b	$1 - \|\eta\|$, $1 + \|\eta\|$
B	see equation (1) and Table 1
C	see equation (1) and Table 1
c	root chord of wing
c_p	pressure coefficient
C_D	drag coefficient
ΔC_D	increment in drag coefficient
C_F	skin friction drag coefficient
D	see equation (1) and Table 1
E	see equation (1) and Table 1
F_1, F_2	defined in equations (16) and (17)
H	δ^*/θ
I_ℓ, J_ℓ	defined in equation (19)
k	y/s
$K(\eta)$	see equation (20) and Table 3
ℓ	index in equation (11)
L	coefficient in equation (11) for δ^*
M	Mach number
n	index in skin friction law Ref.2
P	see equation (1) and Table 1
r	defined by equation (6)
R	Reynolds number = $u_\infty c/\nu_\infty$
R_θ	$u_e\theta/\nu_e$
s	semi-span at trailing edge
S(x)	area of section of wing by plane x = constant
s	distance measured along streamlines in Section 5

T	temperature
u,v	velocity components in x and y directions
U	resultant velocity
V	total volume of wing
x,y,z	Cartesian co-ordinates, x along the centre line, the median plane being $z = 0$.
β	$\sqrt{M^2-1}$
γ	Euler's constant = 0·577216
δ	boundary layer thickness
δ^*	displacement thickness
ε	given by $\eta = 1-\varepsilon$ in equation (13)
η	y/sx
θ	momentum thickness
Θ	$(\theta/c)^{1\cdot 2}$
ν	kinematic viscosity
ϕ	velocity potential
ψ	Euler's ψ function

Subscripts:-

∞	refers to values at infinity
e	refers to values just outside the boundary layer
w	refers to values on the surface of the wing
m	refers to values at a "mean" position

LIST OF REFERENCES

No.	Author	Title, etc.
1	Spence, D.A.	The growth of compressible turbulent boundary layers on isothermal and adiabatic walls. A.R.C. R. & M. 3191. June, 1959.
2	Young, A.D. Kirkby, S.	The profile drag of bi-convex and double wedge wing sections at supersonic speeds. Proceedings of a Symposium on boundary layer effects in aerodynamics held at the N.P.L. (1955). H.M.S.O.
3	Firmin, M.C.P.	Experimental evidence on the drag at zero lift on a series of slender delta wings at supersonic speeds and the drag penalty due to distributed roughness. R.A.E. Technical Note No. Aero 2871, 1963.
4	Cooke, J.C.	An axially symmetric analogue for general three dimensional boundary layers. A.R.C. R. & M. 3200. June, 1959.
5	Weber, J.	Slender delta wings with sharp edges at zero lift. R.A.E. Technical Note No. Aero 2508, ARC 19,549. May, 1957.
6	Monaghan, R.J.	A review and assessment of various formulae for turbulent skin friction in compressible flow. A.R.C. C.P.142. August, 1952.
7	Erdelyi, A. (Ed.)	Higher transcendental functions. Vol.I. McGraw Hill Book Co. Inc. New York, 1953.
8	Davies, H.T.	Tables of higher mathematical functions. Vol.I. Principia Press, Bloomington, 1934.

APPENDIX 1

DETERMINATION OF $\Delta\phi$ AND Δc_p

The equation of the displacement surface is

$$\Delta z = \delta^* = L\left(x - \left|\frac{y}{s}\right|\right)^{\ell} .$$

By Reference 5 we have

$$u_\infty \Delta\phi = \frac{1}{\pi} F_1 + \frac{1}{2\pi} F_2 ,$$

where

$$F_1 = \int_{-sx}^{sx} \frac{\partial \Delta z(x,y')}{\partial x} \log |y-y'| \, dy' , \qquad (16)$$

$$F_2 = \Delta S'(x) \log \tfrac{1}{2}\beta - \int_0^x \Delta S''(x) \log (x-x') \, dx' , \qquad (17)$$

$$\Delta S(x) = 4 \int_0^{sx} \Delta z(x,y) \, dy , \qquad (18)$$

$$\beta^2 = M_\infty^2 - 1 .$$

From equation (18) we have

$$\Delta S(x) = \frac{4Lsx^{\ell+1}}{\ell+1} , \quad \Delta S'(x) = 4Lsx^{\ell} , \quad \Delta S''(x) = 4Ls\ell x^{\ell-1} ,$$

and so

$$F_2 = 4Lsx^{\ell} \log \tfrac{1}{2}\beta - 4Ls\ell \int_0^x x'^{\,\ell-1} \log (x-x') \, dx'$$

$$= 4Lsx^{\ell} \left\{ \log \tfrac{1}{2}\beta - \log x + \gamma + \psi(\ell+1) \right\} ,$$

on putting $x' = tx$ in the integral and noting that, if γ is Euler's constant and $\psi(\ell+1)$ is Euler's ψ function[7],

$$\ell \int_0^1 t^{\ell-1} \log(1-t)\, dt = -\gamma - \psi(\ell+1) .$$

This may be verified by term-by-term integration and the use of the series for $\psi(\ell+1)$[7], namely

$$\psi(\ell+1) = -\gamma + \ell \sum_{n=1}^{\infty} \frac{1}{n(\ell+n)} .$$

Hence

$$\frac{\partial F_2}{\partial x} = 4Ls\ell x^{\ell-1} \left\{ \log \tfrac{1}{2}\beta - \log x + \gamma + \psi(\ell) \right\} ,$$

since

$$\psi(\ell+1) = \frac{1}{\ell} + \psi(\ell) .$$

Now F_1 may be written, putting $y' = sxt'$

$$F_1 = \ell L \int_0^1 sx^{\ell} (1-t')^{\ell-1} \left\{ \log |y-sxt| + \log (y+sxt') \right\} dt'$$

$$= \ell Lsx^{\ell} \int_0^1 t^{\ell-1} \left\{ 2 \log sx + \log |t-a| + \log (b-t) \right\} dt ,$$

on putting

$$t' = 1-t \quad , \quad a = 1-|\eta| \quad , \quad b = 1 + |\eta| \quad , \quad \eta = y/sx .$$

Hence

$$\frac{\partial F_1}{\partial x} = \ell Lsx^{\ell-1} \left\{ 2 \log sx + \frac{2}{\ell} + \ell \int_0^1 t^{\ell-1} \left\{ \log |t-a| + \log (b-t) \right\} dt \right.$$

$$\left. + |\eta| \int_0^1 t^{\ell-1} \left(-\frac{1}{t-a} - \frac{1}{b-t} \right) dt \right\} .$$

On evaluating by parts of the first integral we may reduce this to

$$\frac{\partial F_1}{\partial x} = \ell L s x^{\ell-1}\left[- I_\ell + J_\ell + 2\log|\eta|\right],$$

where

$$I_\ell = \int_0^1 \frac{t^{\ell-1}}{t-a}\,dt \quad , \quad J_\ell = \int_0^1 \frac{t^{\ell-1}}{b-t}\,dt\ . \tag{19}$$

Cauchy principal values are to be taken where necessary.

Hence we have

$$\Delta c_p = -\frac{2u}{u_\infty} = -\frac{2}{u_\infty}\frac{\partial\Delta\phi}{\partial x}$$

$$= \frac{2\ell L s x^{\ell-1}}{\pi}\left\{K(\eta) - 2\log\tfrac{1}{2}\beta s\right\} ,$$

where

$$K(\eta) = I_\ell - J_\ell - 2\log|\eta| - 2\{\gamma + \psi(\ell)\}\ .$$

If $\ell = 4/5$ we find from the tables[8] that

$$\psi(0{\cdot}8) = -0{\cdot}965009 \quad , \quad \gamma = 0{\cdot}577216$$

and hence

$$K(\eta) = I_{0\cdot8} - J_{0\cdot8} - 2\log|\eta| + 0{\cdot}77559\ . \tag{20}$$

$I_{0\cdot8}$ and $J_{0\cdot8}$ may be evaluated numerically for a series of values of η and hence K determined. Table 3 gives values of K for a series of values of η.

If $\eta = 1-\varepsilon$, where ε is small, $K(\eta)$ behaves like $\varepsilon^{-0\cdot2}$; in fact it can be shown that for $\ell = 4/5$

$$K(1-\varepsilon) = 4{\cdot}3240\,\varepsilon^{-0\cdot2} - 5{\cdot}0606 + 0{\cdot}583\varepsilon + O(\varepsilon^2)\ ,$$

and so $K(\eta)$ has an integrable singularity at $\eta = 1$.

W.T.59. K3. Printed in England for H.M. Stationery Office by R.A.E. Farnborough

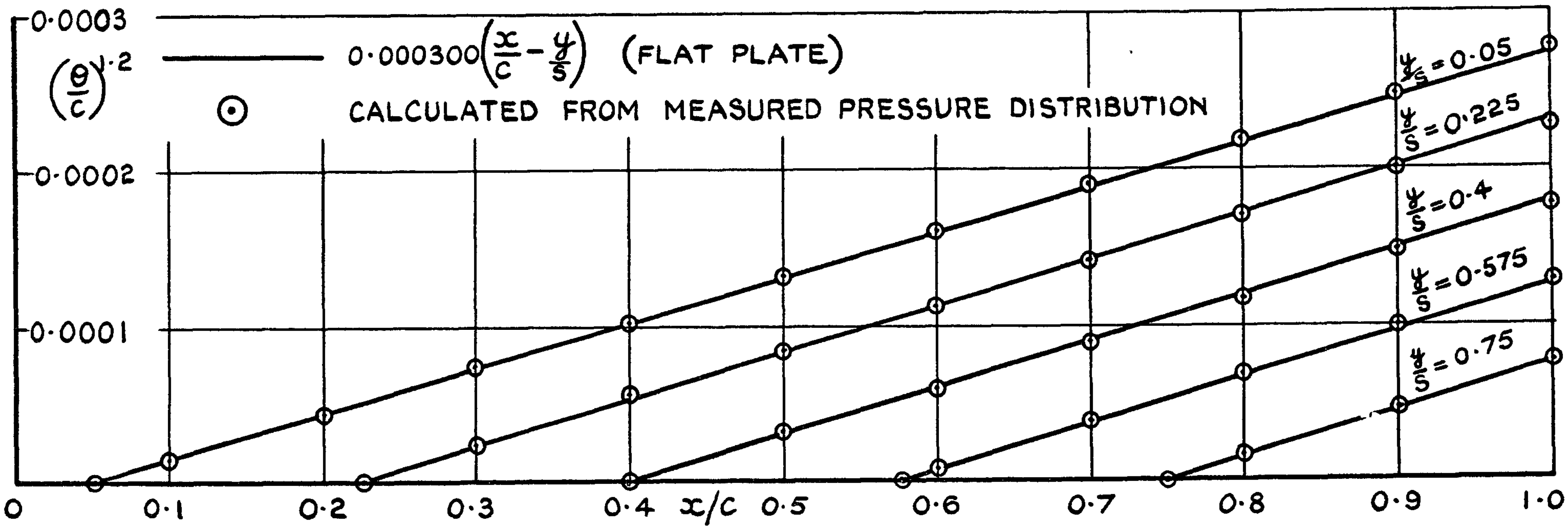

FIG. 1. VALUES OF $(\theta/C)^{1\cdot2}$ BY TWO-DIMENSIONAL CALCULATIONS.

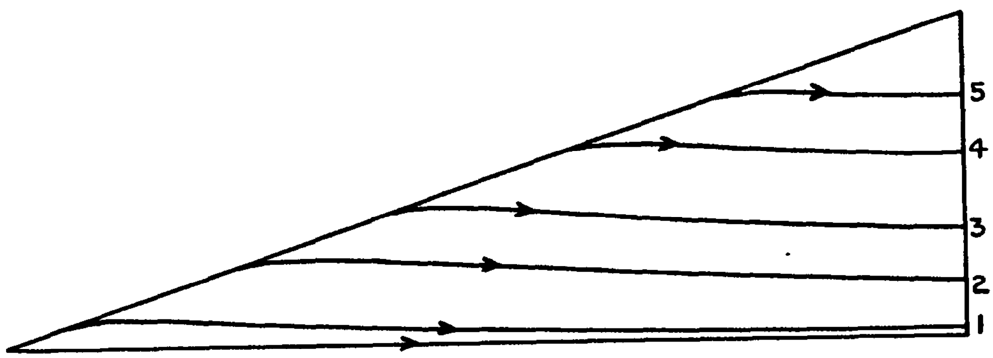

FIG. 2. CALCULATED EXTERNAL STREAMLINES Nos 1–5.

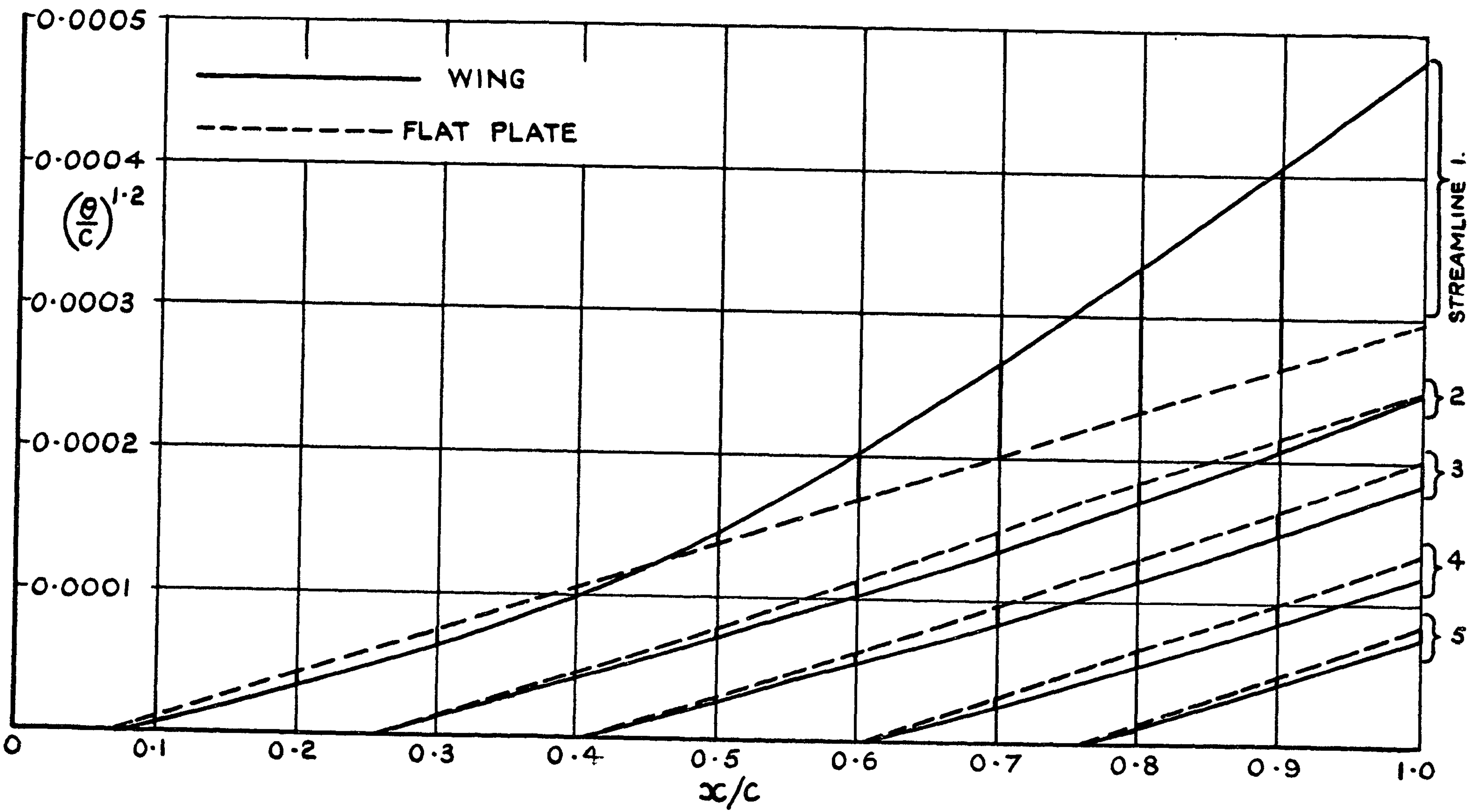

FIG. 3. VALUES OF $(\theta/c)^{1\cdot 2}$ ALONG STREAMLINES 1–5.

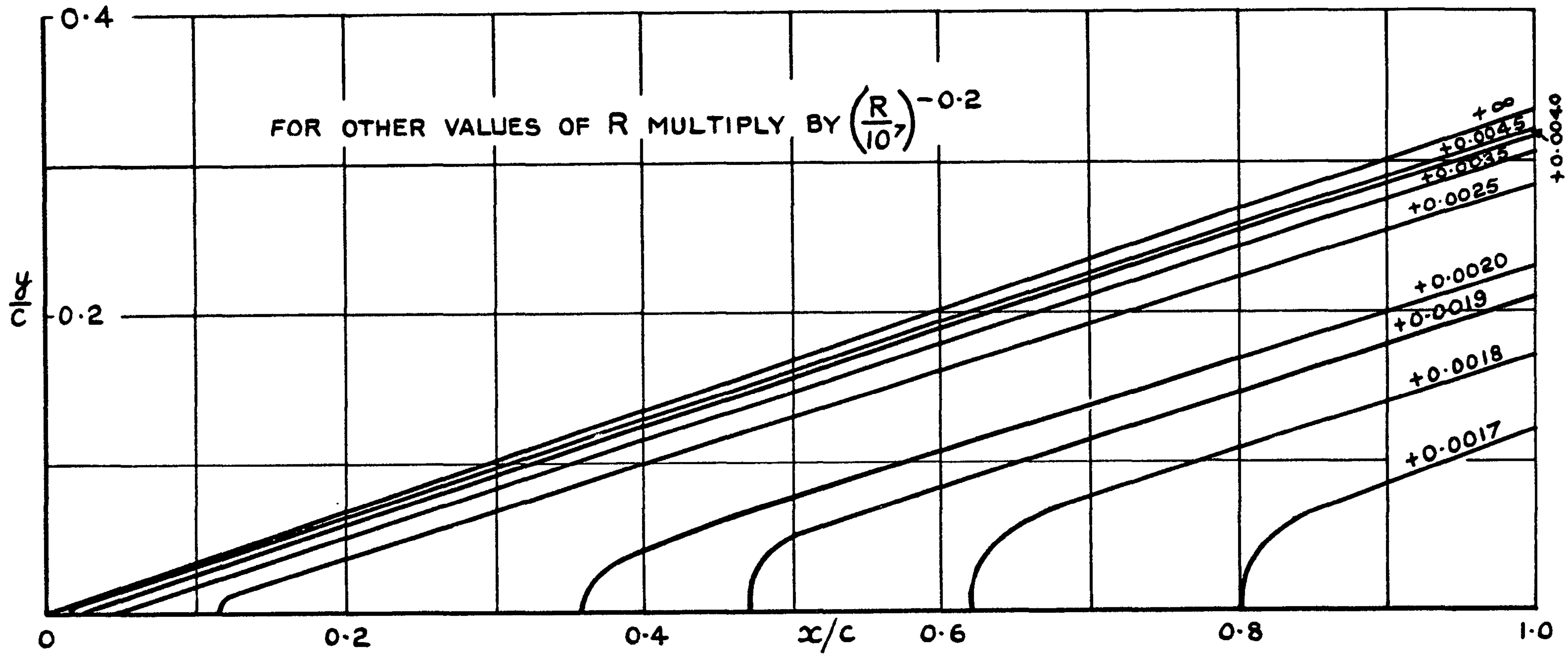

FIG. 4. ISOBARS OF Δc_p FOR $R = 10^7$, $\beta s/c = 0\cdot577$

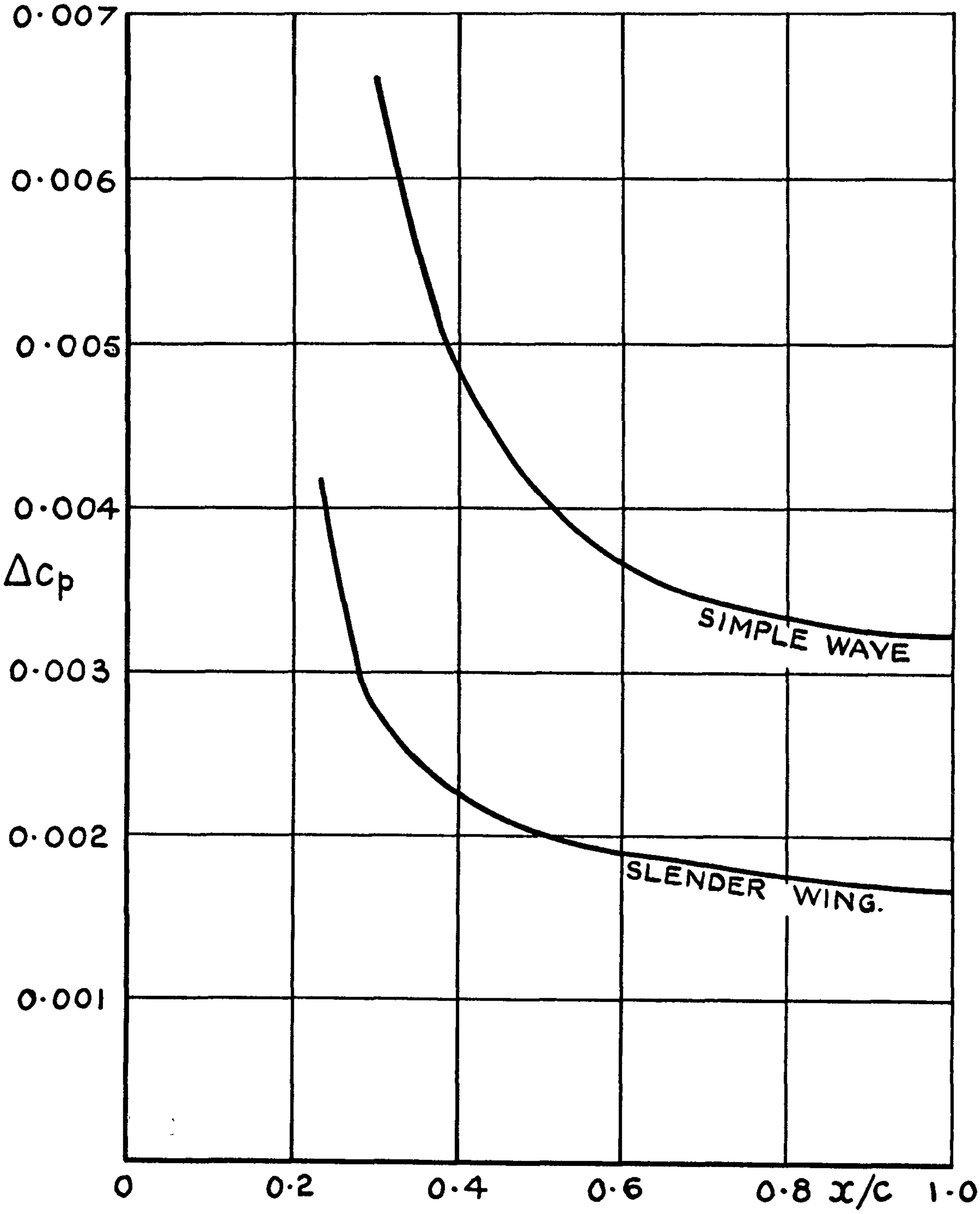

FIG. 5. ΔC_p WHERE $y/s = 0{\cdot}225$, BY SIMPLE WAVE AND SLENDER WING THEORIES.

A.R.C. C.P. No.696

533.693.3 :
532.526.4 :
533.6.011.5

TURBULENT BOUNDARY LAYERS ON DELTA WINGS AT ZERO LIFT.
Cooke, J.C. March, 1963.

It is found that, for turbulent flow at Mach number 2 over a thin delta wing at zero lift, the effect of pressure gradient on the boundary layer is negligible; thus boundary layer calculations allowing for convergence and divergence of streamlines are simplified. When these are done it is found that, except near the centre line, where streamline convergence causes extra thickening towards the trailing edge, the momentum thickness is nearly the same as it would be for flow over a flat plate of the same planform. This enables the boundary layer pressure drag and the skin friction drag to be determined simply. It is found that the pressure drag may be neglected compared with the total drag, whilst the skin friction is the same as that of a flat plate of the same planform.

A.R.C. C.P. No.696

533.693.3 :
532.526.4 :
533.6.011.5

TURBULENT BOUNDARY LAYERS ON DELTA WINGS AT ZERO LIFT.
Cooke, J.C. March, 1963.

It is found that, for turbulent flow at Mach number 2 over a thin delta wing at zero lift, the effect of pressure gradient on the boundary layer is negligible; thus boundary layer calculations allowing for convergence and divergence of streamlines are simplified. When these are done it is found that, except near the centre line, where streamline convergence causes extra thickening towards the trailing edge, the momentum thickness is nearly the same as it would be for flow over a flat plate of the same planform. This enables the boundary layer pressure drag and the skin friction drag to be determined simply. It is found that the pressure drag may be neglected compared with the total drag, whilst the skin friction is the same as that of a flat plate of the same planform.

A.R.C. C.P. No.696

533.693.3 :
532.526.4 :
533.6.011.5

TURBULENT BOUNDARY LAYERS ON DELTA WINGS AT ZERO LIFT.
Cooke, J.C. March, 1963.

It is found that, for turbulent flow at Mach number 2 over a thin delta wing at zero lift, the effect of pressure gradient on the boundary layer is negligible; thus boundary layer calculations allowing for convergence and divergence of streamlines are simplified. When these are done it is found that, except near the centre line, where streamline convergence causes extra thickening towards the trailing edge, the momentum thickness is nearly the same as it would be for flow over a flat plate of the same planform. This enables the boundary layer pressure drag and the skin friction drag to be determined simply. It is found that the pressure drag may be neglected compared with the total drag, whilst the skin friction is the same as that of a flat plate of the same planform.

C.P. No. 696

Published by
HER MAJESTY'S STATIONERY OFFICE

To be purchased from
York House, Kingsway, London w.c.2
423 Oxford Street, London w.1
13A Castle Street, Edinburgh 2
109 St. Mary Street, Cardiff
39 King Street, Manchester 2
50 Fairfax Street, Bristol 1
35 Smallbrook, Ringway, Birmingham 5
80 Chichester Street, Belfast 1
or through any bookseller

S.O. CODE No. 23-9013-96

C.P. No. 696